An Analytical Model for Rapid Estimation of Hurricane Supergradient Winds

Reda Snaiki, Teng Wu*

Department of Civil, Structural and Environmental Engineering, University at Buffalo, Buffalo, NY 14126, USA

*Corresponding author. Email: tengwu@buffalo.edu

Abstract: The supergradient winds that may have severe implications on the wind design of high-rise buildings have been commonly observed in the hurricane boundary layer. However, the widely-used log-law or power-law wind profile excludes the supergradient-wind region in which the tangential winds are larger than the gradient winds. Although high-fidelity, nonlinear hurricane wind models may well capture the supergradient winds, high computational demand is needed for each simulation. Recently developed linear, height-resolving hurricane wind models, while can efficiently consider the existence of supergradient winds, significantly underestimate them due essentially to the ignorance of vertical advection term in the governing equations. A number of studies have actually demonstrated that the vertical advection is a major contributor to the transfer of horizontal momentum to the supergradient region. To this end, a refined analytical model that simultaneously integrates the horizontal advection, vertical advection and vertical diffusion terms into the governing equations is developed for accurately and efficiently estimating the hurricane supergradient winds. The important role of the vertical wind speed in determining the horizontal wind speeds (including supergradient winds) in the hurricane boundary layer is highlighted. Since the horizontal and vertical wind components are mutually dependent, the iteration technique is utilized to solve the proposed analytical model. The consideration of the vertical advection results in intensified supergradient winds that are consistent with the observations. Furthermore, a strong outflow region in the vicinity of the radius of maximum winds due to the supergradient winds can be obtained. Due to its simplicity and computational efficiency, the developed analytical model can be easily implemented in the Monte Carlo simulations for the rapid assessment of hurricane wind risk to coastal structures, especially to high-rise buildings.

Keywords: *Hurricane; Boundary layer; Wind field; Supergradient wind; Vertical advection.*

1. Introduction

Hurricanes are among the most devastating natural hazards responsible for life losses in the coastal regions and massive financial risk to insurance and reinsurance companies (e.g., Pielke et al. 2008; Czajkowski et al., 2011; Rappaport, 2014). The existence of the supergradient-wind region, where the tangential winds are larger than gradient wind, has been widely observed inside the hurricane boundary layer for both marine and landfall conditions (e.g., Giammanco et al. 2012; 2013; He et al. 2013; Tse et al. 2014a; Krupar 2015; Snaiki and Wu 2018a). For example, Franklin et al. (2003), Powell et al. (2003), Bell et al. (2008), Sanger et al. (2014) and Montgomery et al. (2014) confirmed the existence of supergradient winds in the eyewall region of hurricane boundary layer using the GPS dropsondes data provided by the National Oceanic and Atmospheric Administration (NOAA) under marine conditions. A pronounced supergradient-wind region near the radius of maximum winds was also depicted by Vickery et al. (2009) using GPS dropsondes data from 1997 to 2003. On the other hand, Giammanco et al. (2012; 2013) and Krupar (2015) used the velocity Azimuth Display (VAD) technique (Lhermitte and atlas 1961; Browning and Wexler 1968) on the data retrieved by the Weather Surveillance Radar-1988 Doppler (WSR-88D) network to examine the vertical boundary-layer mean wind profile overland. The wind maxima below the gradient wind region was clearly identified near the radius of maximum winds, and the height of supergradient winds was observed to increase with the radial distance from storm center. Similarly, Tse et al. (2014a; 2014b) detected the supergradient-wind region during several typhoons using the measurement data taken by a Doppler Sodar and a boundary layer wind profiler. He et al. (2013) identified the supergradient winds at the height of 500-600 m based on the collected data from Doppler radar profiler. The height range associated with the supergradient winds varies depending on the hurricane intensity and other characteristics. In general, the intense hurricanes present more substantial supergradient winds at relatively lower altitudes (e.g., around 300 m) compared to weak hurricanes. With the development of new lightweight and high-strength materials together with advanced construction techniques, more and more mega-tall buildings have emerged in the coastal areas (Zheng et al. 2019; CTBUH 2020). Hence, it is important to efficiently and accurately take the supergradient region into account in the wind design to ensure target safety of the civil infrastructures (Franklin et al. 2003; Snaiki and Wu 2018b).

The occurrence of supergradient winds requires a sufficient horizontal momentum that is essentially transferred through three processes, namely the horizontal advection, vertical advection and vertical diffusion. The azimuthal frictional wind component is typically negative, however, the supergradient winds mean that a positive azimuthal frictional wind component occurs. Accordingly, the horizontal advection term associated with the azimuthal friction wind component in the governing equation of radial momentum will result in an outflow region associated with the supergradient winds. The slab models widely-utilized in several engineering applications (e.g., Vickery et al. 2000; Vickery et al. 2009), due to the depth-averaging of governing equations, cannot provide accurate assessment of the vertical wind profile (e.g., Kepert 2010a; Kepert 2010b). Hence, significant efforts have been made to develop linear, height-resolving hurricane wind models with parametrization of the turbulent fluxes and surface drag (e.g., Rosenthal 1962; Yoshizumi 1968; Meng et al. 1995, 1997; Kepert 2001; Snaiki and Wu 2017a, 2017b; Fang et al. 2018). However, the pioneering study of Kepert and Wang (2001) demonstrated that these linear hurricane models cannot accurately capture the supergradient winds. In particular, they tend to significantly underestimate the low-level wind maximum (representing the supergradient strength). This shortcoming has been attributed to the neglect of vertical advection that plays an important role in strengthening and sustaining the supergradient wind component.

In this study, a refined analytical model that simultaneously considers the horizontal advection, vertical advection and vertical diffusion will be developed to accurately and efficiently estimate the hurricane supergradient winds. The decomposition method will be utilized in which the wind velocity is expressed as the summation of the gradient-wind and frictional components. Both of these two components are determined analytically by solving the simplified governing equations that include the vertical advection. The importance of the hurricane vertical wind speed in determining its horizontal wind speeds (including supergradient winds) is highlighted. The iteration scheme will be used in the simulations since the horizontal and vertical wind components are mutually dependent. Several hurricane scenarios will be carried out to highlight the significant contributions of the vertical advection to supergradient winds as well as to outflow that occurs above the supergradient region in the vicinity of the radius of maximum winds. The hurricane boundary layer wind profiles obtained from the developed analytical model will be validated based on the observation data from hurricanes Dolly and Ike.

2. Analytical Wind Model

2.1 Theoretical background

The linear analytical wind models of the hurricane boundary layer, due to their simulation convenience and efficiency, have been extensively utilized in engineering applications. These analytical models are typically based on simplified assumptions where only the horizontal advection and vertical diffusion terms are retained while the vertical advection is disregarded. However, the removal of the vertical advection is not supported by results from scale analysis of the fully nonlinear Navier-Stokes equations (Smith 1968; Vogl and Smith 2009; Snaiki and Wu 2017a). In fact all horizontal advection, vertical diffusion and vertical advection components are significant contributors to the supergradient winds in the hurricane boundary layer, as depicted in Fig. 1. More specifically, the substantial increase of the tangential (azimuthal) wind component v_θ associated with supergradient winds essentially result from a high absolute angular momentum M_a ($rv_\theta + fr^2/2$ where f = Coriolis parameter), which is maintained not only through the horizontal advection and vertical diffusion but also through the vertical advection. Furthermore, the vertical advection also contributes towards the outflow as observed above the supergradient-wind region (e.g., Kepert 2001; Kepert and Wang 2001). Since the hurricane vertical wind speed plays an important role in the vertical advection and hence the upward transport of inward momentum from lower altitudes, the maximum winds occur in the eyewall region where the updraft is substantial (e.g., Kepert 2001; Kepert and Wang 2001; Franklin et al. 2003; Powell et al. 2003).

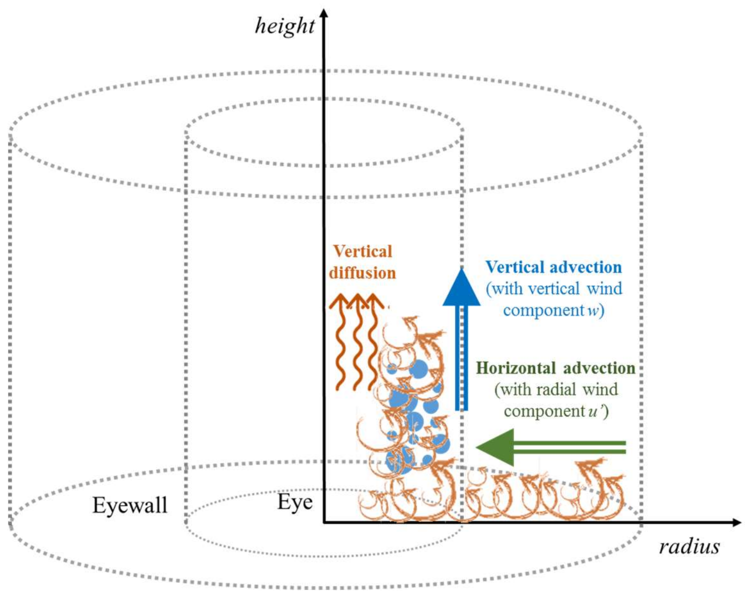

Fig. 1. Schematic illustration for generation mechanism of supergradient winds

The inclusion of the vertical advection term in the governing equations results in a nonlinear wind model (Kepert and Wang 2001). While the nonlinear hurricane model can well predict the supergradient winds (e.g., higher than 10 % of the gradient wind speed near the radius of maximum wind region), its applications is limited due to the high computation demands to obtain the numerical solutions. To reduce the computational cost in the consideration of nonlinear vertical advection terms, the hurricane boundary-layer region will be divided into a series of vertical bins corresponding to various heights. Typically, the change of vertical wind speed within a bin is very small. Hence, it is reasonable to assume a unique vertical wind speed value (radial and azimuthal dependent) within each bin (evaluated at the center of bin). This simplification results in an analytical wind model with the consideration of vertical advection, and hence it offers efficient simulations of more realistic hurricane boundary-layer winds especially in the supergradient-wind region.

2.2 Governing equations

The governing equation of the hurricane boundary-layer wind field can be expressed as follows:

$$\frac{\partial \boldsymbol{v}}{\partial t} + \boldsymbol{v}.\nabla \boldsymbol{v} = -\frac{1}{\rho}\nabla p - f\boldsymbol{k} \times \boldsymbol{v} + \boldsymbol{F} \tag{1}$$

where $\boldsymbol{v}$ = wind velocity; $\boldsymbol{k}$ = unit vector in the vertical direction; f = Coriolis parameter; ρ = air density; $\boldsymbol{F}$ = frictional force; and p = pressure field. The above equations are typically solved with a prescribed pressure distribution in the hurricane boundary layer described as (Holland 1980):

$$p = p_c + \Delta p \exp\left[-\left(r_m / r\right)^B\right] \tag{2}$$

where p_c = central pressure; Δp = central pressure difference; r = radial distance from the tropical cyclone center; r_m = radius of maximum winds; and B = Holland's radial pressure parameter.

To further simplify the calculations of the wind velocity $\boldsymbol{v}$, it is expressed as the vector summation of a gradient wind component in the free atmosphere ($\boldsymbol{v}_g$) and a frictional wind component near the ground surface ($\boldsymbol{v}'$):

$$\boldsymbol{v} = \boldsymbol{v}_g + \boldsymbol{v}' \tag{3}$$

Two separate equations can be obtained based on this decomposition approach:

$$\frac{\partial \boldsymbol{v}_g}{\partial t} + \boldsymbol{v}_g.\nabla \boldsymbol{v}_g = -\frac{1}{\rho}\nabla p - f\boldsymbol{k} \times \boldsymbol{v}_g \tag{4a}$$

$$\frac{\partial \boldsymbol{v}'}{\partial t} + \boldsymbol{v}'.\nabla \boldsymbol{v}' + \boldsymbol{v}'.\nabla \boldsymbol{v}_g + \boldsymbol{v}_g.\nabla \boldsymbol{v}' = -f\boldsymbol{k} \times \boldsymbol{v}' + \boldsymbol{F} \tag{4b}$$

The unsteady term related to the gradient wind can be expressed as $\frac{\partial v_g}{\partial t} = -c\nabla v_g$ (Meng et al. 1995; Snaiki and Wu 2017a; Fang et al. 2018). Consequently, the gradient wind speed (in the azimuthal direction) could be solved straightforwardly in the cylindrical coordinate system (r,θ,z) whose origin is located at the hurricane center (Georgiou 1986; Meng et al. 1995; 1997):

$$v_{\theta g} = \frac{\left(-csin\left(\theta - \upsilon\right) - fr\right)}{2} + \left[\frac{\left(-csin\left(\theta - \upsilon\right) - fr\right)^2}{4} + \frac{r}{\rho}\frac{\partial p}{\partial r}\right]^{1/2} \tag{5}$$

where υ = approach angle (counter clockwise positive from the East); θ = azimuthal angle; and c = hurricane translation speed. The insignificant radial wind component v_{rg} is usually disregarded as suggested by Meng et al. (1995).

For the nonlinear governing equation of Eq. (4b), the scale analysis results in the following equations (Smith and Montgomery 2010; Snaiki and Wu 2017a):

$$u'\frac{\partial u'}{\partial r} + \frac{v_{\theta g} + v'}{r}\frac{\partial u'}{\partial \theta} + w\frac{\partial u'}{\partial z} - \frac{v'^2}{r} - \xi_g v' = K\frac{\partial^2 u'}{\partial z^2} \tag{6a}$$

$$u'\frac{\partial v'}{\partial r} + \frac{v_{\theta g} + v'}{r}\frac{\partial v'}{\partial \theta} + w\frac{\partial v'}{\partial z} + \frac{u'v'}{r} + \xi_{ag}u' + \frac{v'}{r}\frac{\partial v_{\theta g}}{\partial \theta} = K\frac{\partial^2 v'}{\partial z^2} \tag{6b}$$

where u' and v' are frictional components of the radial and azimuthal wind speeds, respectively; $\xi_g = {}^{2v_{\theta g}}\!/_{r} + f$ is the absolute angular velocity; $\xi_{ag} = {}^{\partial v_{\theta g}}\!/_{\partial r} + {}^{v_{\theta g}}\!/_{r} + f$ is the vertical component of absolute vorticity of gradient wind; and K represents eddy viscosity. For engineering purposes, the nonlinear equations could be further simplified by disregarding all derivatives with respect to the angular coordinate θ (e.g., Meng et al. 1995; 1997). Accordingly, only the nonlinear terms corresponding to the vertical advections, namely $w\frac{\partial u'}{\partial z}$ and $w\frac{\partial v'}{\partial z}$ are retained in the simulation of hurricane boundary-layer winds. The newly obtained equations can be expressed as:

$$w\frac{\partial u'}{\partial z} - \left(2\frac{v_{\theta g}}{r} + f\right)v' = K\frac{\partial^2 u'}{\partial z^2} \tag{7a}$$

$$w\frac{\partial v'}{\partial z} + \left(\frac{\partial v_{\theta g}}{\partial r} + \frac{v_{\theta g}}{r} + f\right)u' = K\frac{\partial^2 v'}{\partial z^2} \tag{7b}$$

2.3 Analytical solutions

By introducing a new variable $\omega = \sqrt{\frac{\beta}{\alpha}}u' + iv'$, Eqs. (7a) and (7b) can be unified into one simple equation as:

$$\frac{\partial^2 \omega}{\partial z^2} - \frac{w}{K}\frac{\partial \omega}{\partial z} - 2i\sqrt{\alpha\beta}\,\omega = 0 \tag{8}$$

where $\alpha = \frac{1}{2K}\xi_g$ and $\beta = \frac{1}{2K}\xi_{ag}$. To obtain the analytical solutions of the governing equations involving nonlinear vertical advection terms, the hurricane boundary-layer region is divided into a series of vertical bins corresponding to various heights. The vertical wind speed $w(r,\theta)$ for each bin can be determined based on the iteration process as will be highlighted subsequently.

The characteristic equation of the second-order differential equation (Eq. 8) can be extracted as:

$$q_k^2 - \frac{w}{K}q_k - 2i\sqrt{\alpha\beta} = 0 \tag{9}$$

The roots of the auxiliary equation $\left(q_k\right)$ are determined and expressed in terms of the parameters x and y:

$$x = \sqrt{{w^2}/{2K^2} + \sqrt{{w^4}/{4K^4} + 16\alpha\beta}} \tag{10a}$$

$$y = \frac{4\sqrt{\alpha\beta}}{x} \tag{10b}$$

Accordingly, the solution of q_k to ensure the perturbations of v' and u' equal to zero at very high altitudes (i.e., $\boldsymbol{v'}\big|_{z'\to\infty} = 0$) (Smith and Montgomery 2010) is given as:

$$q_k = \left({}^{w}\!/_{2K} - {}^{x}\!/_{2} \right) - {}^{iy}\!/_{2} \tag{11}$$

Hence, the solution of Eq. (8) can be obtained as follows:

$$\omega = (D_1 + iD_2)\exp\left[\left({}^{w}\!/_{2K} - {}^{x}\!/_{2} \right) z - {}^{iyz}\!/_{2} \right] \tag{12}$$

where D_1 and D_2 are two constants. They are determined using the boundary condition above the ground surface as:

$$\rho K \frac{\partial \boldsymbol{v'}}{\partial z}\bigg|_{z'=0} = \rho C_d \left|\boldsymbol{v_s}\right| \boldsymbol{v_s} \tag{13}$$

where $\boldsymbol{v_s}$ = total wind velocity near the ground surface; and C_d = drag coefficient. Therefore, the frictional wind components are determined as:

$$u' = \sqrt{{}^{\alpha}\!/_{\beta}}\exp\left[\left({}^{w}\!/_{2K} - {}^{x}\!/_{2} \right) z \right]\left[D_1 \cos\left({}^{yz}\!/_{2} \right) + D_2 \sin\left({}^{yz}\!/_{2} \right) \right] \tag{14a}$$

$$v' = \exp\left[\left({}^{w}\!/_{2K} - {}^{x}\!/_{2} \right) z \right]\left[-D_1 \sin\left({}^{yz}\!/_{2} \right) + D_2 \cos\left({}^{yz}\!/_{2} \right) \right] \tag{14b}$$

where D_1 and D_2 are given as:

$$D_1 = {C_d \left|\boldsymbol{v}_s\right| \left\{ \sqrt{\frac{\beta}{\alpha}} \left[\left(\frac{w}{2K} - \frac{x}{2} \right) - C_d \frac{\left|\boldsymbol{v}_s\right|}{K} \right] v_{rg} - \frac{y}{2} v_{\theta g} \right\}} \Bigg/ {K \left\{ \frac{y^2}{4} + \left[\left(\frac{w}{2K} - \frac{x}{2} \right) - C_d \frac{\left|\boldsymbol{v}_s\right|}{K} \right]^2 \right\}} \tag{15a}$$

$$D_2 = {\left\{ \frac{y}{2} D_1 + \frac{C_d \left|\boldsymbol{v}_s\right|}{K} v_{\theta g} \right\}} \Bigg/ {\left\{ \left(\frac{w}{2K} - \frac{x}{2} \right) - C_d \frac{\left|\boldsymbol{v}_s\right|}{K} \right\}} \tag{15b}$$

The vertical wind speed w is needed to obtain the frictional wind components, and it will be calculated based on the continuity equation which can be expressed in the cylindrical coordinates as:

$$\frac{1}{r}\frac{\partial(ru')}{\partial r}+\frac{\partial w}{\partial z}=0 \tag{16}$$

Accordingly, the vertical wind component can be obtained as:

$$w=-\frac{1}{r}\frac{\partial}{\partial r}\left(r\int_0^z u'dz\right) \tag{17}$$

Since the vertical wind speed w depends on the frictional wind u' (radial component), which is itself dependent on w, the iteration approach is utilized in the computation. Figure 2 presents a flowchart for calculating the height-resolving, hurricane boundary-layer winds in this study. First, initial estimates of the vertical wind speed w_0 can be obtained using Eq. (17) where the radial wind component is determined without consideration of the vertical advection. Once the initial value of w is given, the corresponding frictional wind components could be evaluated based on Eqs. (14a), (14b), (15a) and (15b). The vertical wind speed will be updated to be w_{i+1} until $|w_{i+1}-w_i|<\varepsilon$ is achieved, where ε is a selected threshold. Two to three iterations are typically needed with a prescribed threshold $\varepsilon=5\%$ for all simulations in the present study. It should be noted that w at very low altitudes (near surface) is negligible compared to that near and above the supergradient region (e.g., Kepert and Wang 2001; Vogl 2009).

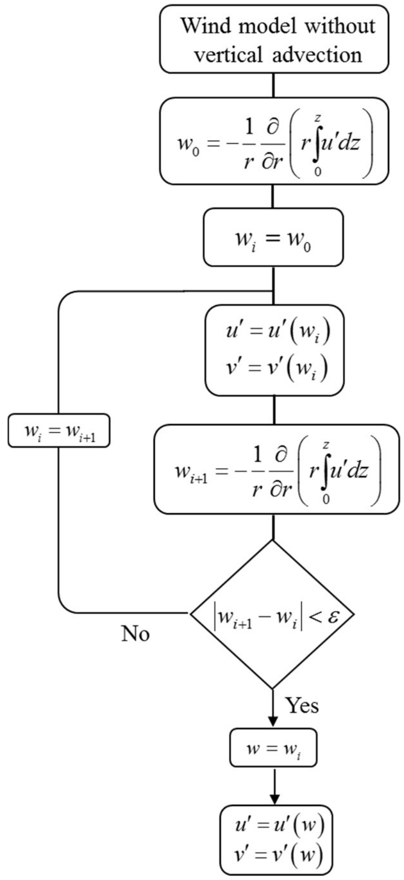

Fig. 2. Flow chart of hurricane boundary-layer wind simulation

3. Model Validation and Application

3.1 Model validation

The developed refined analytical model for effectively simulating hurricane boundary-layer winds will be validated based on two scenarios, namely hurricane Dolly (2008) and hurricane Ike (2008). In both simulation scenarios, the vertical bins are discretized with $\Delta z = 100\,m$.

Hurricane Dolly caused widespread power outages and substantial tree damage in Texas with approximately \$1.05 billion of total loss (Pasch and Kimberlain 2009). Dolly reached hurricane strength on 23 July 2008 and made landfall at South Padre Island on 23 July at 1800 UTC as a Category 1 hurricane with a maximum sustained surface wind speed of 39 m/s. After landfall, Dolly weakened and moved along the Texas-Mexico border. The minimum pressure recorded during hurricane Dolly was estimated to be 963 hpa around 1400 UTC on the July 23rd with a maximum sustained surface wind of 44 m/s. The comparison of the wind profiles at the location of (N25.91°, W97.42°) calculated based on the analytical wind models with and without consideration of the vertical advection is depicted in Fig. 3, together with the measured data from the KBRO Doppler radar (Krupar 2015). All necessary parameters needed in the simulations were obtained from the HURDAT database on 23 July 2008. As shown in the figure, the simulation accuracy of the supergradient winds associated with Hurricane Dolly is significantly improved by considering the vertical advection in the analytical wind model.

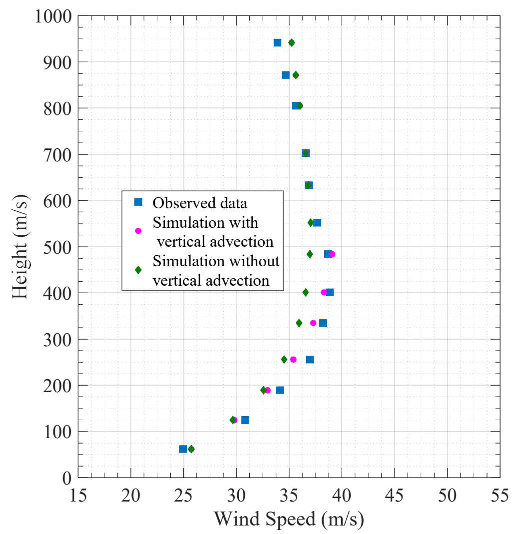

Fig. 3. Observed and simulated wind speed of Hurricane Dolly (2008)

Hurricane Ike caused many deaths and extensive damage along the Caribbean and the coastlines of Texas and Louisiana. It reached Category 4 hurricane with an estimated central pressure of 935 hpa and a maximum sustained surface wind of 65 m/s at 0600 UTC on September 4th. Hurricane Ike first made landfall in Cuba then entered the Gulf of Mexico. It made landfall again near Houston, Texas, at 0700 UTC on September 13th after which it quickly weakened to a tropical storm. Figure 4 presents the comparison of the wind profiles at the location of (N29.47°, W95.07°) provided by the analytical wind models with and without consideration of the vertical advection, together with the observed data from the KHGX Doppler radar (Krupar 2015). All required parameters for the wind field simulations were obtained from the HURDAT database on 13 September 2008. As shown in the figure, the simulation accuracy of the supergradient winds associated with Hurricane Ike is greatly improved by considering the vertical advection in the analytical wind model.

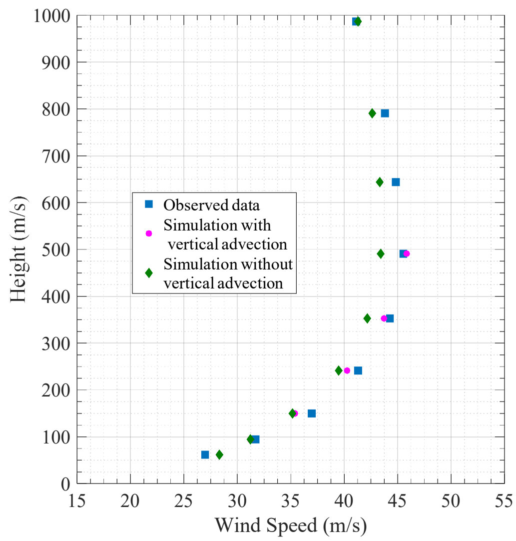

Fig. 4. Observed and simulated wind speed of Hurricane Ike (2008)

The proposed analytical model is further compared to the linear model of Meng et al. (1995) and the semi-empirical model of Vickery et al. (2009) for a hurricane scenario with storm parameters of $p_c = 960\,\text{hpa}$, $r_m = 60\,\text{km}$, $B = 1.0$, $c = 7.5\,\text{m/s}$, $\upsilon = 90°$, $\psi = 32.8°$ and $z_0 = 0.001\,\text{m}$. Figure 5 depicts the hurricane mean wind profiles near the radius of maximum wind. As shown in the figure, both models of the present study and Vickery et al. (2009) provide significantly improved simulation of supergradient winds compared to the linear model of Meng et al. (1995) (without consideration of vertical advection). It should be noted that the semi-empirical model of Vickery et al. (2009) is mostly well-suited for marine conditions (Snaiki and Wu 2018a). The simplification of a constant vertical wind speed for each bin is also well justified based on the results of this numerical example. For example, the vertical wind speeds at 600 m and 700 m are 0.238 m/s and 0.251 m/s, respectively. The vertical wind speed of 0.246 m/s at the center of the corresponding bin (with a size of 100 m) is selected as the unique value. Accordingly, the change in the vertical wind speed within this bin is less than 5% with respect to the employed constant value. Further improved simulation accuracy can be always achieved by reducing the bin size.

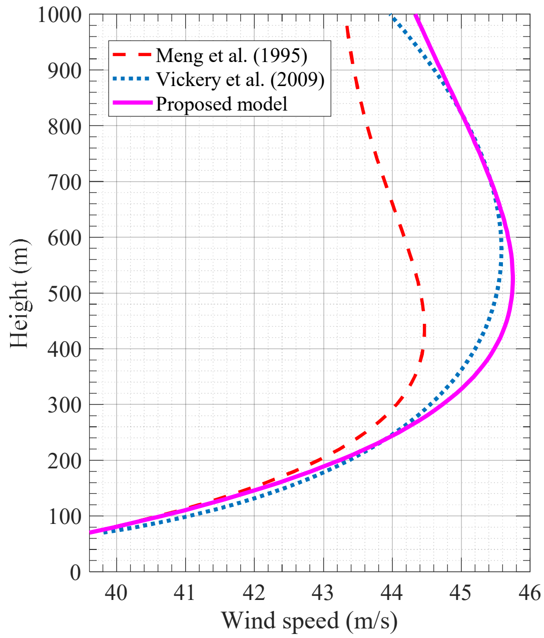

Fig. 5. Comparison of hurricane mean wind profiles at $\theta = 0°$ obtained using various models

3.2 Application

A case study will be presented in this section to comprehensively investigate the vertical advection effects on the simulated hurricane boundary-layer winds. The storm parameters of the selected hurricane scenario, namely the central pressure p_c, radius of maximum winds r_m, Holland parameter B, translation speed c, approach angle υ, latitude ψ, and surface roughness z_0 are listed in Table 1.

Table 1. Storm parameters for hurricane boundary-layer wind simulation

Parameter	p_c(hpa)	r_m(km)	B	c(m/s)	υ(°)	ψ(°)	z_0(m)
value	950	60	1.3	5	90	32.8	0.01

Figure 6 depicts the hurricane mean wind profiles at three different locations near the radius of the maximum winds, namely $r = 40\text{km}$, $r = 50\text{km}$, $r = 60\text{km}$ under various values of vertical wind speed w. For the sake of illustration, a unique value of w is imposed on the whole hurricane boundary-layer region to highlight its effects on the mean wind profile. As shown in the figures, the height of the maximum winds increases with radius in accordance with the observations and numerical simulations (e.g., Zhang et al. 2011; Snaiki and Wu 2017a).

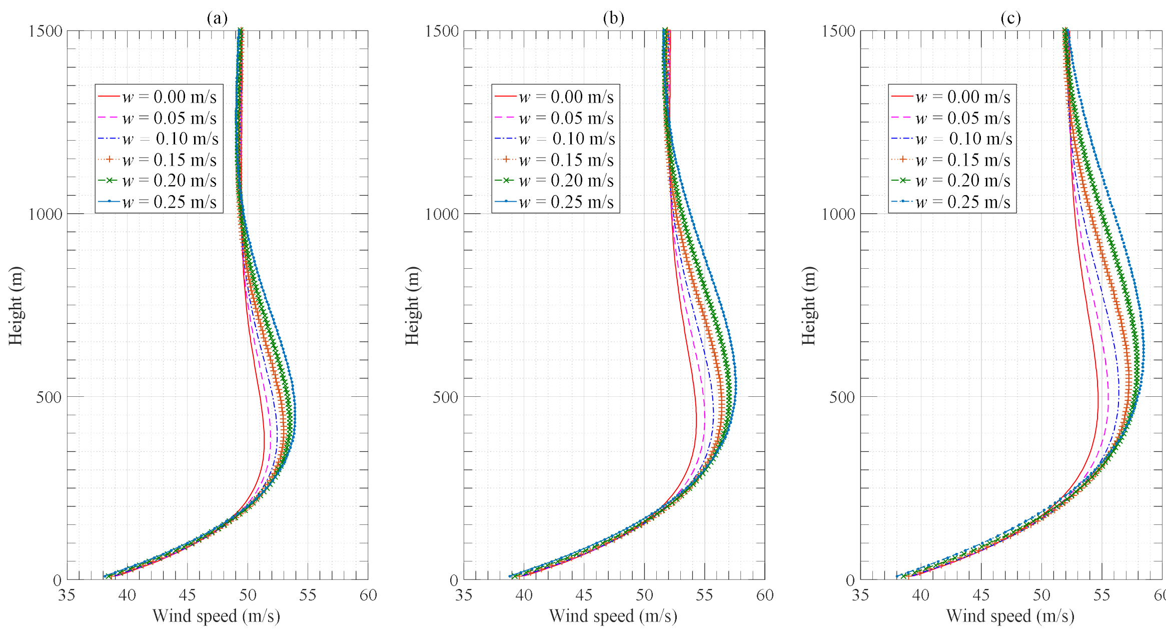

Fig. 6. Hurricane mean wind profiles at different locations: (a) r =40 km; (b) r =50 km; (c) r = 60 km

The comparison of supergradient strengths, defined as the relative change between the maximum supergradient-wind and corresponding gradient-wind speeds, indicates that the supergradient winds become more significant with enhancement of the vertical advection. For instance, the supergradient strength is equal to 12.04 % under the strong vertical advection with $w = 0.25$ m/s while it is equal to 5.15 % without consideration of vertical advection ($w = 0 m/s$). Table 2 summarizes the obtained supergradient strengths at different wind profile locations for various values of the vertical wind speed w.

Table 2. Comparison of supergradient strengths for various vertical wind speed values

	$w = 0.00$ m/s	$w = 0.05$ m/s	$w = 0.10$ m/s	$w = 0.15$ m/s	$w = 0.20$ m/s	$w = 0.25$ m/s
$r = 40$ km	4.30 %	5.36 %	6.48 %	7.57 %	8.61 %	9.52 %
$r = 50$ km	4.66 %	6.67 %	8.07 %	9.43 %	10.65 %	11.66 %
$r = 60$ km	5.15 %	6.80 %	8.46 %	10.06 %	11.41 %	12.40 %

The contours of the hurricane boundary-layer winds for two cases of $w = 0.00$ m/s and $w = 0.15$ m/s are plotted in Fig. 7 to further examine the vertical advection effects on the wind spatial distribution. A strong supergradient-wind region is clearly identified near the radius of maximum winds when considering the vertical advection.

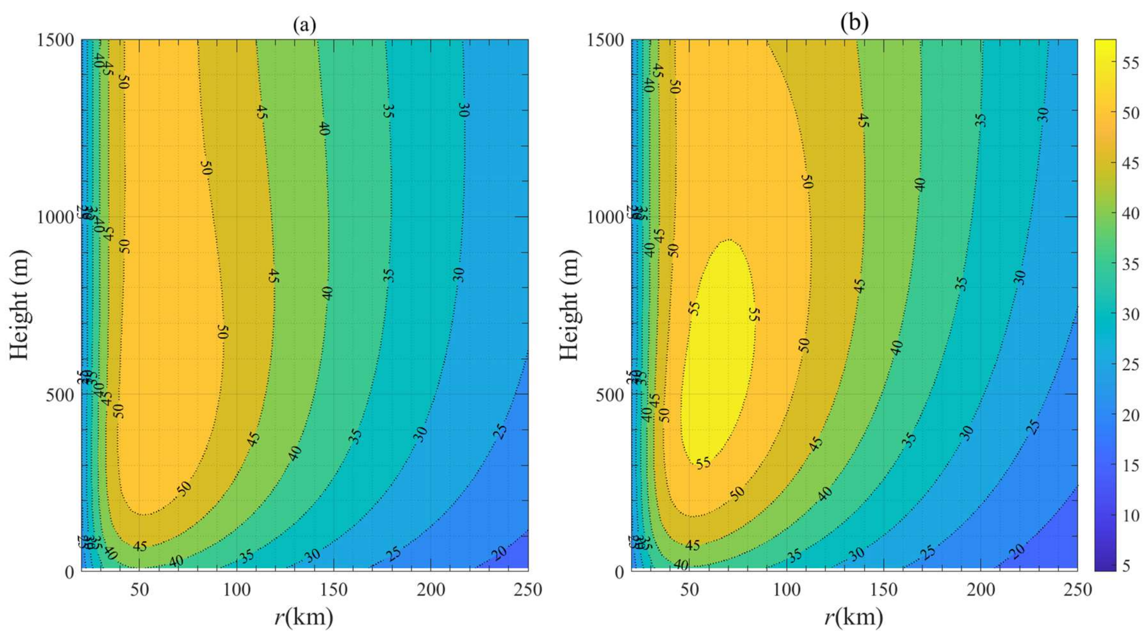

Fig. 7. Contour of wind field for the cases: (a) $w = 0.00$ m/s (without vertical advection); (b) $w = 0.15$ m/s (with vertical advection)

As discussed in the preceding section, the consideration of vertical advection in the vicinity of the radius of maximum winds results in an outflow region (e.g., Kepert and Wang 2001). This phenomenon is illustrated using the hurricane radial wind profiles as shown in Fig. 8, where the height of outflow region generally increases with the radius.

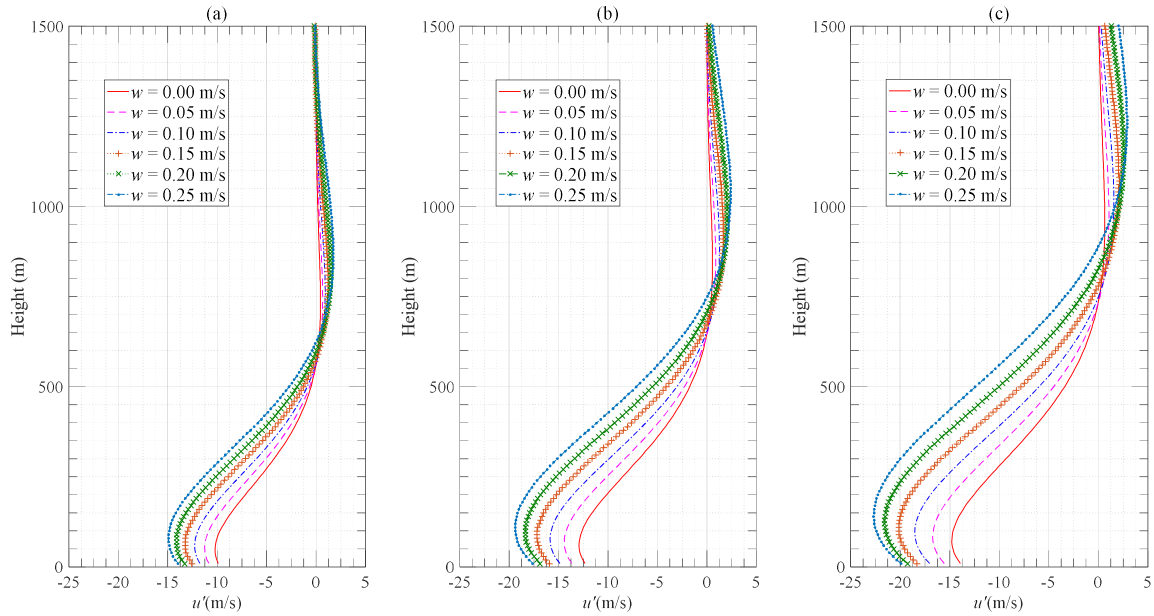

Fig. 8. Hurricane radial wind profiles at different locations: (a) r =40 km; (b) r =50 km; (c) r = 60 km

A detailed comparison of the maximum outflow for various values of vertical wind speed is summarized in Table 3. It is shown that the outflow strength is positively proportional to the vertical wind speed. For instance, the outflow at the radius $r = 60\,\mathrm{km}$ is equal to 2.9 m/s for the case of $w = 0.25$ m/s, more than four times the value for the case of $w = 0\,m/s$ (without consideration of the vertical advection). This observation indicates that the gradient-wind height will be significantly underestimated if the vertical advection is not considered in the simulation of hurricane boundary-layer winds.

Table 3. Comparison of outflow speeds for various vertical wind speed values

	$w = 0.00$ m/s	$w = 0.05$ m/s	$w = 0.10$ m/s	$w = 0.15$ m/s	$w = 0.20$ m/s	$w = 0.25$ m/s
$r = 40\,\mathrm{km}$	0.44	0.67	0.93	1.21	1.48	1.74
$r = 50\,\mathrm{km}$	0.56	0.88	1.27	1.67	2.06	2.40
$r = 60\,\mathrm{km}$	0.64	1.06	1.60	2.08	2.55	2.90

4. Concluding Remarks

An inherent shortcoming of the widely-used linear hurricane wind models is that the vertical advection is not considered, and hence an underestimated, weak low-level wind maximum (representing the supergradient strength) is typically obtained. In this study, a refined analytical model that simultaneously considers the horizontal advection, vertical diffusion and vertical advection is developed for accurately and efficiently estimating hurricane supergradient winds. The iteration scheme is utilized in the computational scheme since the horizontal and vertical wind components are mutually dependent. It has been demonstrated that the vertical advection plays an important role in strengthening and maintaining the supergradient winds. The supergradient strength obtained from the proposed analytical wind model with consideration of vertical advection are typically higher than 10%, while the values simulated by using the conventional linear hurricane models are generally lower than 5%. Due to the consideration of vertical advection, the high simulation accuracy of the developed analytical model for the hurricane supergradient winds is validated with the observation data. In addition, the consideration of vertical advection results in an outflow region near the radius of maximum winds, and hence an increased gradient-wind height.

Acknowledgments

The support for this project provided by the NSF Grant # CMMI 15-37431 is gratefully acknowledged.

References

Bell, M.M. and Montgomery, M.T., 2008. Observed structure, evolution, and potential intensity of category 5 Hurricane Isabel (2003) from 12 to 14 September. Monthly Weather Review, 136(6), pp.2023-2046.

Browning, K.A. and Wexler, R., 1968. The determination of kinematic properties of a wind field using Doppler radar. Journal of Applied Meteorology, 7(1), pp.105-113.

CTBUH (The Council on Tall Buildings and Urban Habitat): Global Tall Building Database, 2020. http://www.skyscrapercenter.com/, accessed on March. 25th, 2020.

Czajkowski, J., Simmons, K. and Sutter, D., 2011. An analysis of coastal and inland fatalities in landfalling US hurricanes. Natural hazards, 59(3), pp.1513-1531.

Fang, G., Zhao, L., Cao, S., Ge, Y. and Pang, W., 2018. A novel analytical model for wind field simulation under typhoon boundary layer considering multi-field correlation and height-dependency. Journal of Wind Engineering and Industrial Aerodynamics, 175, pp.77-89.

Franklin, J.L., Black, M.L. and Valde, K., 2003. GPS dropwindsonde wind profiles in hurricanes and their operational implications. Weather and Forecasting, 18(1), pp.32-44.

Georgiou, P.N., 1986. Design wind speeds in tropical cyclone-prone regions. PhD Thesis University of Western Ontario, London, Ontario, Canada.

Giammanco, I.M., Schroeder, J.L. and Powell, M.D., 2012. Observed characteristics of tropical cyclone vertical wind profiles. Wind and Structures, 15(1), p.65.

Giammanco, I.M., Schroeder, J.L. and Powell, M.D., 2013. GPS dropwindsonde and WSR-88D observations of tropical cyclone vertical wind profiles and their characteristics. Weather and Forecasting, 28(1), pp.77-99.

He, Y.C., Chan, P.W. and Li, Q.S., 2013. Wind profiles of tropical cyclones as observed by Doppler wind profiler and anemometer. Wind and Structures, 17(4), pp.419-433.

Holland, G.J., 1980. An analytic model of the wind and pressure profiles in hurricanes. Monthly weather review, 108(8), pp.1212-1218.

Kepert, J., 2001. The dynamics of boundary layer jets within the tropical cyclone core. Part I: Linear theory. Journal of the Atmospheric Sciences, 58(17), pp.2469-2484.

Kepert, J. and Wang, Y., 2001. The dynamics of boundary layer jets within the tropical cyclone core. Part II: Nonlinear enhancement. Journal of the atmospheric sciences, 58(17), pp.2485-2501.

Kepert, J.D., 2010a. Slab-and height-resolving models of the tropical cyclone boundary layer. Part I: Comparing the simulations. Quarterly Journal of the Royal Meteorological Society, 136(652), pp.1686-1699.

Kepert, J.D., 2010b. Slab-and height-resolving models of the tropical cyclone boundary layer. Part II: Why the simulations differ. Quarterly Journal of the Royal Meteorological Society, 136(652), pp.1700-1711.

Krupar III, R.J., 2015. Improving surface wind estimates in tropical cyclones using WSR-88D derived wind profiles (Doctoral dissertation).

Lhermitte, R., and D. Atlas, 1961. Precipitation motion by pulse Doppler radar. Proc. 9th Wea Radar Conf., Boston, MA, Am. Meteor. Soc., 218-223.

Meng, Y., Matsui, M. and Hibi, K., 1995. An analytical model for simulation of the wind field in a typhoon boundary layer. Journal of Wind Engineering and Industrial Aerodynamics, 56(2-3), pp.291-310.

Meng, Y., Matsui, M. and Hibi, K., 1997. A numerical study of the wind field in a typhoon boundary layer. Journal of Wind Engineering and Industrial Aerodynamics, 67, pp.437-448.

Montgomery, M.T., Zhang, J.A. and Smith, R.K., 2014. An analysis of the observed low-level structure of rapidly intensifying and mature hurricane Earl (2010). Quarterly Journal of the Royal Meteorological Society, 140(684), pp.2132-2146.

Pasch, R. J., and T. B. Kimberlain, 2009: Tropical cyclone report: Hurricane Dolly (AL042008). National Hurricane Center, 19 pp. [Available online at http://www.nhc.noaa.gov/pdf/TCR-AL042008_Dolly.pdf.]

Pielke Jr, R.A., Gratz, J., Landsea, C.W., Collins, D., Saunders, M.A. and Musulin, R., 2008. Normalized hurricane damage in the United States: 1900–2005. Natural Hazards Review, 9(1), pp.29-42.

Powell, M.D., Vickery, P.J. and Reinhold, T.A., 2003. Reduced drag coefficient for high wind speeds in tropical cyclones. Nature, 422(6929), pp.279-283.

Rappaport, E.N., 2014. Fatalities in the United States from Atlantic tropical cyclones: New data and interpretation. Bulletin of the American Meteorological Society, 95(3), pp.341-346.

Rosenthal, S.L., 1962. A theoretical analysis of the field of motion in the hurricane boundary layer.

Sanger, N.T., Montgomery, M.T., Smith, R.K. and Bell, M.M., 2014. An observational study of tropical cyclone spinup in Supertyphoon Jangmi (2008) from 24 to 27 September. Monthly Weather Review, 142(1), pp.3-28.

Smith, R.K., 1968. The surface boundary layer of a hurricane. Tellus, 20(3), pp.473-484.

Smith, R.K. and Montgomery, M.T., 2010. Hurricane boundary-layer theory. Quarterly Journal of the Royal Meteorological Society, 136(652), pp.1665-1670.

Snaiki, R. and Wu, T., 2017a. A linear height-resolving wind field model for tropical cyclone boundary layer. Journal of Wind Engineering and Industrial Aerodynamics, 171, pp.248-260.

Snaiki, R. and Wu, T., 2017b. Modeling tropical cyclone boundary layer: Height-resolving pressure and wind fields. Journal of Wind Engineering and Industrial Aerodynamics, 170, pp.18-27.

Snaiki, R. and Wu, T., 2018a. A semi-empirical model for mean wind velocity profile of landfalling hurricane boundary layers. Journal of Wind Engineering and Industrial Aerodynamics, 180, pp.249-261.

Snaiki, R. and Wu, T., 2018b, April. An Improved Methodology for Risk Assessment of Tropical Cyclones under Changing Climate. In 33rd Conference on Hurricanes and Tropical Meteorology. AMS, May, Ponte Verda, FL, USA.

Tse, K.T., Li, S.W., Lin, C.Q. and Chan, P.W., 2014a. Wind characteristics observed in the vicinity of tropical cyclones: An investigation of the gradient balance and super-gradient flow. Wind and Structures, 19(3), pp.249-270.

Tse, K.T., Li, S.W. and Fung, J.C.H., 2014b. A comparative study of typhoon wind profiles derived from field measurements, meso-scale numerical simulations, and wind tunnel physical modeling. Journal of Wind Engineering and Industrial Aerodynamics, 131, pp.46-58.

Vickery, P.J., Skerlj, P.F., Steckley, A.C. and Twisdale, L.A., 2000. Hurricane wind field model for use in hurricane simulations. Journal of Structural Engineering, 126(10), pp.1203-1221.

Vickery, P.J., Wadhera, D., Powell, M.D. and Chen, Y., 2009. A hurricane boundary layer and wind field model for use in engineering applications. Journal of Applied Meteorology and Climatology, 48(2), pp.381-405.

Vogl, S., 2009. Tropical Cyclone Boundary-Layer Models (Doctoral dissertation, lmu).

Vogl, S. and Smith, R.K., 2009. Limitations of a linear model for the hurricane boundary layer. Quarterly Journal of the Royal Meteorological Society: A journal of the atmospheric sciences, applied meteorology and physical oceanography, 135(641), pp.839-850.

Yoshizumi, S., 1968. On the asymmetry of wind distribution in the lower layer in typhoon. Journal of the Meteorological Society of Japan. Ser. II, 46(3), pp.153-159.

Zhang, J.A., Rogers, R.F., Nolan, D.S. and Marks Jr, F.D., 2011. On the characteristic height scales of the hurricane boundary layer. Monthly Weather Review, 139(8), pp.2523-2535.

Zheng, C., Liu, Z., Wu, T., Wang, H., Wu, Y. and Shi, X., 2019. Experimental investigation of vortex-induced vibration of a thousand-meter-scale mega-tall building. Journal of Fluids and Structures, 85, pp.94-109.